Published in IET Communications
Received on 1st November 2012
Revised on 28th December 2013
Accepted on 3rd February 2014
doi: 10.1049/iet-com.2013.0710

ISSN 1751-8628

Adaptive schemes and analysis for blind beamforming with insufficient cyclic prefix in single carrier-frequency division multiple access systems

Kuo-Ching Fu, Shiuan-Wei Huang, Yung-Fang Chen
Communication Engineering Department, National Central University, Taiwan
E-mail: yfchen@ce.ncu.edu.tw

Abstract: When the duration of the cyclic prefix (CP) is shorter than that of the channel impulse response in single carrier-frequency division multiple access systems, inter-symbol interference and inter-carrier interference will degrade the system performance. Previously, one solution of this problem while considering the effect of carrier frequency offsets (CFOs) and the co-channel interference is a blind received beamforming scheme based on eigenanalysis in a batch mode. As the capability in suppressing the multipath signal with the delay larger than the CP length has not previously been analysed theoretically for the scheme, the theoretical analysis regarding the capability in suppressing the long-delayed multipath signal is provided in this study. The analysis provided in this study is also utilised to design an adaptive processing scheme. The adaptive algorithm is developed to find the beamforming weight vector updated on a per symbol basis without using reference signals. The proposed adaptive algorithm reduces the computational complexity of and shows competitive performance under the insufficient CP, the CFOs, the co-channel interference and the time-varying scenarios. The simulation results reveal that the proposed adaptive algorithm provides better performance than the previously proposed algorithm.

1 Introduction

Single carrier-frequency division multiple access (SC-FDMA) is adopted for uplink transmission in Evolved-Universal Terrestrial Radio Access Network (E-UTRAN) [1]. Its low peak-to-average power ratio feature is suitable for mobile devices [2]. When the duration of the cyclic prefix (CP) is larger than the channel impulse response duration, it only needs a single-tap equaliser to deal with multipath channel problems in orthogonal frequency division multiplexing (OFDM) [3], orthogonal frequency division multiple access (OFDMA) and SC-FDMA systems. When the duration of the CP is shorter than the channel impulse response duration, inter-symbol interference (ISI) and inter-carrier interference (ICI) will degrade the system performance. The normal CP and the extended CP modes are two configurations for the uplink transmission in E-UTRAN [4]. The extended CP mode can be selected for long multipath channel environments, but transmission rates or bandwidth efficiency would be reduced. If the normal CP mode is employed under the insufficient CP condition, error rates will increase.

Recently, in order to provide better bandwidth efficiency, a few results have been published for dealing with the effects of the insufficient CP. The related research results for OFDM systems can be found in [5–9]. On the other hand, antenna arrays may be utilised to improve system performance [10, 11]. A beamforming scheme is proposed to cancel co-channel interference by utilising virtual carriers [12] without considering the effect of frequency offsets and merely for single user OFDM systems. The beamforming schemes in [13–15] are also proposed to suppress co-channel interference for OFDM systems. Besides, an adaptive beamforming algorithm is presented to combat the co-channel interference problem using pilot symbols for an OFDM system [16].

There are several techniques proposed to mitigate ISI and ICI effectively [17, 18] under various considerations for OFDM-based systems. In particular, the work of [17] utilises null subcarriers for the design of the frequency domain equaliser to suppress channel induced interference such as ICI and ISI with insufficient guard interval. However, the ability of the wideband interference suppression is not provided and the method may need a long training sequences. The method is designed for single user systems. The extension for the multiple antenna case has not been demonstrated yet. For OFDMA systems, when the length of the channel impulse response is longer than the length of the CP, there would be residual inter-block interference and the performance of OFDMA degrades. An approach to mitigate the problem is to use a time-domain equaliser. In [18], a carrier nulling-based algorithm is presented by treating pilot subcarriers similarly as unused null subcarriers for the design. With the use of the time-domain equaliser, the advantage of the simple modulation/demodulation process through discrete-Fourier-transform (DFT)/inverse DFT (IDFT) operations diminishes for OFDM-based systems.

In addition to the solutions for OFDM systems, there are some research results in dealing with the problem for single carrier CP systems. A weight control method based on the maximisation of the signal-to-interference plus noise ratio (SINR) at the discrete frequency domain equaliser output has been proposed in [19]. In [20], it uses directional beamforming and artificial delay to dynamically adjust the channel impulse response within the time duration of the cyclic extension. In [21], the paper proposed a minimum-mean-square error-based equaliser, which jointly performs equalisation and carrier frequency offsets (CFOs) compensation. Note that none of the above methods deals with the combination of the problems regarding the ISI and ICI because of insufficient CP, strong wideband co-channel interferers, lack of reference signals and frequency offset conditions. A blind beamforming scheme for the insufficient CP problem in SC-FDMA systems has been proposed in [22]. Without using reference signals, this scheme can cancel ISI along with ICI, and strong wideband co-channel interferers under frequency offset scenarios in the system. It achieves competitive performances under the normal CP mode. By considering the effect of CFOs, the blind scheme utilises the least squares (LS) criteria [23] to deal with frequency synchronisation errors in calculating the beamforming weight vector. In [24], the paper proposes a power amplifier subcarrier interference cancellation method to overcome the distortion because of high peak-to-average power ratio (PAPR) characteristic in OFDM-based systems.

In [22], basically, based on generalised eigenvalue decomposition (GED) analysis, the beamforming weight vector $\boldsymbol{w}$ is the largest generalised eigenvector of the signal-plus-interference (plus noise) spatial correlation matrix $\boldsymbol{R}_{S+I}$ and the interference-alone (plus noise) spatial correlation matrix $\boldsymbol{R}_I$. The mathematical expression is

$$\boldsymbol{R}_{S+I}\boldsymbol{w} = \lambda_{\max}\boldsymbol{R}_I\boldsymbol{w} \tag{1}$$

where $\lambda_{\max}$ is the largest generalised eigenvalue. In this method, the spatial correlation matrices have to be estimated by using received samples in one or a few data blocks and the GED operation is performed as in a batch fashion. In [22], the interference-alone (plus noise) spatial correlation matrix is estimated by averaging one block data using all samples at the zero-valued subcarriers in a batch mode. In this manner, the data length of one block may not provide an accurate estimate. Even though one frame data may provide enough data length to obtain accurate estimates in stationary channels, however, the channel gains usually fluctuate in the propagation environments across several blocks within one frame, especially in high mobility scenarios. Furthermore, the proposed algorithm provides lower computational complexity than [22] and the proposed adaptive algorithm provides better performance than the previously proposed algorithms.

GED analysis can be used widely in various applications, for example, blind source separation, noise cancellation, antenna array weight estimation, statistical parameter estimation, neural networks etc. GED analysis is usually applied with the SINR maximisation criterion in the signal process field. The related methods with the GED analysis can be found in the literature [25–28]. In this paper, the signal processing scheme in [22] to form the spatial correlation matrices are analysed for the verification of the suppression of the multipath with the delay larger than the CP duration. The analysis is also utilised to design an adaptive processing scheme. The novel adaptive processing scheme is developed to solve the blind beamforming problem under consideration. The proposed algorithm updates the weight vector adaptively when the new SC-FDMA symbol comes in so that the weight vector is calculated inherently with accumulating information of the previous data blocks. To develop an adaptive algorithm for the blind beamforming scheme is not straightforward. For example, there are many snapshots per each SC-FDMA symbol with different characteristics. Based on the analysis regarding the CFO effect because of the long-delay multipath for the beamforming problem under consideration, not all samples at the zero-valued subcarriers (virtual carriers) should be used for processing in terms of performance and computational cost. Compared to the batch processing-based method in [22], which finds the largest generalised eigenvector of the spatial correlation matrices of the current block as the beamforming weight vector, the adaptive algorithm improves the performance in time-varying channels with reduced computational cost.

2 System model and blind beamforming

The procedures of the SC-FDMA transceiver are described as follows. The block diagram of the SC-FDMA transceiver is shown in Fig. 1 [2].

Let $\boldsymbol{x}^{(v)}(k) = \left[x_0^{(v)}(k), x_1^{(v)}(k), \ldots, x_{N^{(v)}-1}^{(v)}(k)\right]^{\mathrm{T}}$ be an $N^{(v)} \times 1$ column vector representing the kth block of the vth user for transmission in SC-FDMA communication systems, where $x_i^{(v)}(k)$ denotes the ith information symbol of the vth user in the kth block, T denotes the transpose operation, the value of $N^{(v)}$ is the total number of subcarriers which are used by the vth user, and the (v) in superscript stands for the vth user throughout this paper. $N_o^{(v)}$ denotes the starting subcarrier index of the vth user, which will be used in the later derivation. After applying the $N^{(v)}$-point DFT operations to $\boldsymbol{x}^{(v)}(k)$, the frequency domain signal of the $N^{(v)} \times 1$ $\boldsymbol{X}^{(v)}(k)$ vector is produced. It then maps $\boldsymbol{X}^{(v)}(k)$ to subchannel $\gamma^{(v)}$ which is assigned to the vth user, where the subchannel means several neighbouring workable resource blocks in the system, and each resource block contains 12 consecutive subcarriers in the E-UTRAN uplink [4]. Let $\boldsymbol{\Gamma}^{(v)}$ be a set of subcarrier indexes of the used subchannel for the vth user and M is the number of points for the following IDFT operation. Subsequently, by padding $M - N^{(v)}$ zeros in the specified positions for virtual carriers and being multiplied by the amplitude scaling factor, the $N^{(v)} \times 1$ vector $\boldsymbol{X}^{(v)}(k)$ is converted to a data stream that is represented as an $M \times 1$ vector $\tilde{\boldsymbol{X}}^{(v)}(k)$. After performing the M-point IDFT operation on $\tilde{\boldsymbol{X}}^{(v)}(k)$ and adding the CP with the length of N_g, the data are sent out.

For an antenna array of Q elements, the $Q \times 1$ quasi-stationary channel impulse response of the vth user of the discrete-time version is expressed as

$$\begin{aligned}\boldsymbol{h}_d^{(v)}(k) &= [\,h_{d(1)}^{(v)}(k),\quad h_{d(2)}^{(v)}(k),\quad \ldots,\quad h_{d(Q)}^{(v)}(k)\,]^{\mathrm{T}} \\ &= \sum_{i=1}^{L_d^{(v)}} \alpha_i^{(v)}(k)\boldsymbol{a}(\theta_i^{(v)})\delta(d - d_i^{(v)})\end{aligned} \tag{2}$$

where $\alpha_i^{(v)}(k)$ is the ith path complex gain, $d_i^{(v)}$ is the ith path time delay relative to the arrival time of the first path, $L_d^{(v)}$ is the total number of multipaths for the vth user and $\boldsymbol{a}(\theta_i^{(v)})$

IET Commun., 2014, Vol. 8, Iss. 9, pp. 1477–1487
doi: 10.1049/iet-com.2013.0710

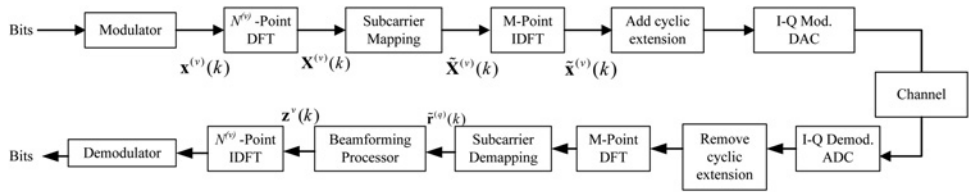

Fig. 1 *Block diagram of the SC-FDMA transceiver*

denotes an array response from the ith path with an angle-of-arrival (AOA) $\theta_i^{(v)}$.

After the removal of the CP and the M-point DFT operation, we have the following equation for the kth transmission block (one SC-FDMA symbol) of the qth antenna output for $q = 1, \ldots, Q$:

$$\begin{aligned}\tilde{\boldsymbol{r}}^{(q)}(k) = \sum_{v=1}^{V} \sqrt{P^{(v)}}\Big(&\boldsymbol{W}_{\text{FFT}}\boldsymbol{C}^{(v)}\boldsymbol{H}_{U(q)}^{(v)}(k)\boldsymbol{W}_{\text{IFFT}}\tilde{\boldsymbol{X}}^{(v)}(k)\\ &+ \boldsymbol{W}_{\text{FFT}}\boldsymbol{C}^{(v)}\boldsymbol{H}_{\text{ICI}(q)}^{(v)}(k)\boldsymbol{W}_{\text{IFFT}}\tilde{\boldsymbol{X}}^{(v)}(k)\\ &+ \boldsymbol{W}_{\text{FFT}}\boldsymbol{C}^{(v)}\boldsymbol{H}_{\text{ISI}(q)}^{(v)}(k)\boldsymbol{W}_{\text{IFFT}}\tilde{\boldsymbol{X}}^{(v)}(k-1)\\ &+ \boldsymbol{n}^{(q)}(k)\end{aligned} \tag{3}$$

where V is the total number of users, $\sqrt{P^{(v)}}$ is related to the transmission power of the vth user, $\boldsymbol{C}^{(v)} = \text{diag}(1, \mathrm{e}^{\mathrm{j}2\pi\Delta_f^{(v)}/M}, \ldots, \mathrm{e}^{\mathrm{j}2\pi\Delta_f^{(v)}(M-1)/M})$ denotes the matrix of CFO components of the vth user after removing CP and $\Delta_f^{(v)}$ is the normalised CFO of the vth user. $\boldsymbol{W}_{\text{FFT}}$ is the M-point DFT matrix with the (i, j)th component $[\boldsymbol{W}_{\text{FFT}}]_{i,j} = (1/\sqrt{M})\exp(-j2\pi(i-1)(j-1)/M)$ in the ith row and in the jth column; $\boldsymbol{W}_{\text{IFFT}}$ is the M-point inverse DFT matrix with $\boldsymbol{W}_{\text{IFFT}} = \boldsymbol{W}_{\text{FFT}}^{\text{H}}$; H denotes the Hermitian transpose operation; and $\boldsymbol{n}^{(q)}(k)$ denotes the additive white Gaussian noise (AWGN). The $M \times M$ matrices, $\boldsymbol{H}_{U(q)}^{(v)}(k)$, $\boldsymbol{H}_{\text{ICI}(q)}^{(v)}(k)$ and $\boldsymbol{H}_{\text{ISI}(q)}^{(v)}(k)$, are the channel matrices of the qth antenna according to the vth user. $\boldsymbol{H}_{U(q)}^{(v)}(k)$ is the channel matrix whose time delays are shorter than the duration of the CP. On the contrary, $\boldsymbol{H}_{\text{ICI}(q)}^{(v)}(k)$ and $\boldsymbol{H}_{\text{ISI}(q)}^{(v)}(k)$ mean the channel matrices whose time delays are greater than the duration of the CP. The channel matrices are given as follows (see (4))

(see (5))

$$\boldsymbol{H}_{U(q)}^{(v)}(k) = \begin{bmatrix} h_{0(q)}^{(v)}(k) & 0 & \ddots & \ddots & 0 & h_{N_g(q)}^{(v)}(k) & \cdots & h_{1(q)}^{(v)}(k) \\ & \ddots & 0 & \ddots & \ddots & 0 & \ddots & \vdots \\ \vdots & & h_{0(q)}^{(v)}(k) & \ddots & \ddots & \ddots & \ddots & h_{N_g(q)}^{(v)}(k) \\ & \vdots & & \ddots & \ddots & 0 & \ddots & 0 \\ & & \vdots & & \ddots & \ddots & \ddots & \vdots \\ h_{N_g(q)}^{(v)}(k) & & & \vdots & & \ddots & \ddots & \\ \vdots & \ddots & & & \vdots & & \ddots & 0 \\ 0 & \cdots & h_{N_g(q)}^{(v)}(k) & & & \cdots & & h_{0(q)}^{(v)}(k) \end{bmatrix} \tag{4}$$

$$\boldsymbol{H}_{\text{ICI}(q)}^{(v)}(k) = \begin{bmatrix} 0 & \cdots & \cdots & \cdots & 0 & 0 & \ddots & 0 \\ \vdots & \ddots & \ddots & \ddots & \vdots & h_{N_g+1(q)}^{(v)}(k) & \ddots & \vdots \\ 0 & & \ddots & \ddots & 0 & \vdots & \ddots & 0 \\ h_{N_g+1(q)}^{(v)}(k) & \ddots & \ddots & \ddots & \ddots & h_{d_T^{(v)}(q)}^{(v)}(k) & \ddots & h_{N_g+1(q)}^{(v)}(k) \\ \vdots & \ddots & 0 & \ddots & \ddots & 0 & \ddots & \vdots \\ h_{d_T^{(v)}(q)}^{(v)}(k) & \vdots & h_{N_g+1(q)}^{(v)}(k) & \ddots & \ddots & \ddots & \ddots & h_{d_T^{(v)}(q)}^{(v)}(k)0 \\ \vdots & \ddots & \vdots & \ddots & 0 & \ddots & \ddots & \vdots \\ 0 & \cdots & h_{d_T^{(v)}(q)}^{(v)}(k) & \cdots & \ddots & 0 & \cdots & 0 \end{bmatrix} \tag{5}$$

and

$$
\boldsymbol{H}_{\mathrm{ISI}(q)}^{(v)}(k)=\begin{bmatrix} 0 & \cdots & h_{d_T^{(v)}(q)}^{(v)}(k-1) & \cdots & h_{2(q)}^{(v)}(k-1) \\ \vdots & \ddots & 0 & \ddots & \vdots \\ 0 & \cdots & \ddots & \cdots & h_{d_T^{(v)}(q)}^{(v)}(k-1) \\ \vdots & \vdots & \vdots & \ddots & \vdots \\ 0 & \cdots & 0 & \cdots & 0 \end{bmatrix} \tag{6}
$$

where $d_T^{(v)}$ is the maximum time delay of the multipath with the value larger than the CP length. The related derivation can be found in [22, 17]. We assume the CFO values of the vth user among all transmit/receive antenna pairs are the same [29].

The blind beamforming scheme [22] is briefly described as follows. First, it utilises the method in [23] with the LS criteria to mitigate the CFO effect of each antenna before calculating the beamforming weight vector. The output of the qth antenna after compensating CFOs can be expressed as

$$
\boldsymbol{G}^{(q)}(k)=(\tilde{\boldsymbol{\Pi}}^{\mathrm{H}}\tilde{\boldsymbol{\Pi}})^{-1}\tilde{\boldsymbol{\Pi}}^{\mathrm{H}}\boldsymbol{r}^{(q)}(k) \tag{7}
$$

where $\tilde{\boldsymbol{\Pi}}$ is a $\xi' \times \xi'$ CFO interference matrix with the component $[\tilde{\boldsymbol{\Pi}}]_{i,j}=\sum_{n=0}^{M-1}\exp\left\{\mathrm{j}2\pi\left[(j-i)+\Delta_f^{(v)}\right]n/M\right\}$ in the ith row and the jth column and assume zero-valued subcarriers having 'zero-valued' CFOs. $\boldsymbol{r}^{(q)}(k)=\left[\tilde{r}_{\boldsymbol{\Phi}(1)}^{(q)}(k), \tilde{r}_{\boldsymbol{\Phi}(2)}^{(q)}(k), \ldots, \tilde{r}_{\boldsymbol{\Phi}(\xi')}^{(q)}(k)\right]^{\mathrm{T}}$ is a $\xi' \times 1$ vector, where $\xi'=\xi+\phi$ is the total number of the subcarriers; $\xi=\sum_{v=1}^{V} N^{(v)}$ is the total number of subcarriers which are used for transmission for all users; ϕ is the number of the zero-valued subcarriers which are used for estimating interference-alone spatial correlation matrix; $\tilde{r}_{\boldsymbol{\Phi}(l)}^{(q)}(k)$ is the $\boldsymbol{\Phi}(l)$th component of $\boldsymbol{r}^{(q)}(k)$, and $\boldsymbol{\Phi}(l)$ means the value of the lth element in $\boldsymbol{\Phi}$. $\boldsymbol{\Phi}=\boldsymbol{\Gamma}\cup\boldsymbol{\Psi}$ where $\boldsymbol{\Gamma}=\cup_{v=1}^{V}\boldsymbol{\Gamma}^{(v)}$ is the index set of all subcarriers which are used for transmission and $\boldsymbol{\Psi}$ is the set of the indexes of the zero-valued subcarriers in the guard bands.

Next, the spatial correlation matrices of the batch processing-based method, the estimated signal-plus-interference (plus noise) spatial correlation matrix and the estimated interference (plus noise) spatial correlation matrix, are calculated for the vth user as

$$
\tilde{\boldsymbol{R}}_{S+I}^{(v)}(k)=\frac{1}{N^{(v)}}\sum_{l=N_0^{(v)}}^{N_0^{(v)}+N^{(v)}-1}\boldsymbol{g}_l(k)\boldsymbol{g}_l^{\mathrm{H}}(k) \tag{8}
$$

and

$$
\tilde{\boldsymbol{R}}_{I}^{(v)}(k)=\frac{1}{\varphi}\left(\sum_{l=N_0^{(v)}-\varphi/2}^{N_0^{(v)}-1}\boldsymbol{g}_l(k)\boldsymbol{g}_l^{\mathrm{H}}(k)+\sum_{l=N_0^{(v)}+N^{(v)}}^{N_0^{(v)}+N^{(v)}+\varphi/2-1}\boldsymbol{g}_l(k)\boldsymbol{g}_l^{\mathrm{H}}(k)\right) \tag{9}
$$

where $N_0^{(v)}$ denotes the starting subcarrier index of the vth user, $N^{(v)}$ is the total number of the subcarriers which are used by the vth user as defined before, and $\boldsymbol{g}_l(k)=\left[\boldsymbol{G}_{(l)}^{(1)}(k), \boldsymbol{G}_{(l)}^{(2)}(k), \ldots, \boldsymbol{G}_{(l)}^{(Q)}(k)\right]^{\mathrm{T}}$ is the $Q\times 1$ spatial snapshot at the lth subcarrier after compensating CFOs in (7).

Finally, it finds the beamforming weight vector based on the following criterion as

$$
\underset{\boldsymbol{w}^{(v)}(k)}{\text{Maximise}}\ \frac{\boldsymbol{w}^{(v)}(k)^{\mathrm{H}}\tilde{\boldsymbol{R}}_{S+I}^{(v)}(k)\boldsymbol{w}^{(v)}(k)}{\boldsymbol{w}^{(v)}(k)^{\mathrm{H}}\tilde{\boldsymbol{R}}_{I}^{(v)}(k)\boldsymbol{w}^{(v)}(k)} \tag{10}
$$

where the $Q\times 1$ weight vector $\boldsymbol{w}^{(v)}(k)$ is the largest generalised eigenvector of the resulting matrix pencil $\{\tilde{\boldsymbol{R}}_{S+I}^{(v)}(k), \tilde{\boldsymbol{R}}_{I}^{(v)}(k)\}$ for the solution of the criterion (10). The beamforming weight vector is applied at the samples across all of the assigned subcarriers for the vth user.

3 Analysis for the suppression capability of the self-interference

The term 'self-interference' means that the interference is generated because of the insufficient duration of the CP or caused by longer delay of multipath of the desired user's signal, instead of the interference from other users. In [22], the ability of the multipath suppression is not analysed and the analysis is provided in this section. There are many snapshots per each SC-FDMA symbol with different characteristics. The analysis explains why we select samples to perform the estimation of the correlation matrix related to the proposed adaptive algorithm.

In this section, the signal processing scheme in [22] to form the spatial correlation matrices are analysed for the verification of the suppression of the multipath with the delay larger than the CP duration. To evaluate the effect of ICI caused by insufficient CP, the channel matrices in the time domain are used to obtain the frequency response matrices which are adapted from [30] for OFDM systems. It can be utilised to analyse the beamforming problem as the beamforming algorithm is performed before the $N^{(v)}$-point DFT operations. The property obtained in the analysis is also utilised for the design of the proposed adaptive algorithm.

$\boldsymbol{H}_{U(q)}^{f(v)}(k)=\boldsymbol{W}_{\mathrm{FFT}}\boldsymbol{H}_{U(q)}^{(v)}(k)\boldsymbol{W}_{\mathrm{IFFT}}$ is the frequency response matrix of the useful part for the vth user where f and (v) in the superscript of the matrix $\boldsymbol{H}_{U(q)}^{f(v)}(k)$ denote the frequency domain and the index of a user, respectively. The element in the mth row and the nth column of $\boldsymbol{H}_{U(q)}^{f(v)}(k)$ is given as

$$
\begin{aligned}
\left[\boldsymbol{H}_{U(q)}^{f(v)}(k)\right]_{m,n} &= \frac{1}{M}\sum_{d=0}^{N_g} h_{d(q)}^{(v)}(k)\,\mathrm{e}^{-\mathrm{j}2\pi dn/M}\sum_{r=0}^{M-1}\mathrm{e}^{\mathrm{j}2\pi r(n-m)/M} \\
&= \begin{cases} \sum_{d=0}^{N_g} h_{d(q)}^{(v)}(k)\,\mathrm{e}^{-\mathrm{j}2\pi dm/M}, & m=n \\ 0, & m\neq n \end{cases}
\end{aligned} \tag{11}
$$

$\boldsymbol{H}_{\mathrm{ICI}(q)}^{f(v)}(k)=\boldsymbol{W}_{\mathrm{FFT}}\boldsymbol{H}_{\mathrm{ICI}(q)}^{(v)}(k)\boldsymbol{W}_{\mathrm{IFFT}}$ is the frequency response matrix of the ICI part for the vth user, and the element in

doi: 10.1049/iet-com.2013.0710

the mth row and the nth column of $\boldsymbol{H}^{f(v)}_{\mathrm{ICI}(q)}(k)$ is derived as

$$\left[\boldsymbol{H}^{f(v)}_{\mathrm{ICI}(q)}(k)\right]_{m,n} = \frac{1}{M}\sum_{d=N_g+1}^{d_T^{(v)}} h^{(v)}_{d(q)}(k)\,\mathrm{e}^{-\mathrm{j}2\pi dn/M}\sum_{r=d-N_g}^{M-1}\mathrm{e}^{\mathrm{j}2\pi r(n-m)/M} \quad (12)$$

$\boldsymbol{H}^{f(v)}_{\mathrm{ISI}(q)}(k) = \boldsymbol{W}_{\mathrm{FFT}}\boldsymbol{H}^{(v)}_{\mathrm{ISI}(q)}(k)\boldsymbol{W}_{\mathrm{IFFT}}$ is the frequency response matrix of the ISI part for the vth user, and the element in the mth row and the nth column of $\boldsymbol{H}^{f(v)}_{\mathrm{ISI}(q)}(k)$ is given as

$$\left[\boldsymbol{H}^{f(v)}_{\mathrm{ISI}(q)}(k)\right]_{m,n} = \frac{1}{M}\sum_{d=N_g+1}^{d_T^{(v)}} h^{(v)}_{d(q)}(k-1)\,\mathrm{e}^{-\mathrm{j}2\pi(d-N_g)n/M}\sum_{r=0}^{d-N_g-1}\mathrm{e}^{\mathrm{j}2\pi r(n-m)/M} \quad (13)$$

Referring to (3), $\boldsymbol{H}^{f(v)}_{U(q)}(k)$ comprising the multipath components with the delays smaller than the CP duration is a diagonal matrix so that the signal of a particular subcarrier does not leak into the others. If the samples at a particular zero-values subcarrier from multiple antennas are constructed to form the spatial snapshot, the spatial statistics will not contain the spatial information of the useful part.

On the other hand, the off-diagonal elements of $\boldsymbol{H}^{f(v)}_{\mathrm{ICI}(q)}(k)$ and $\boldsymbol{H}^{f(v)}_{\mathrm{ISI}(q)}(k)$ because of the multipath components with the delays larger than the CP duration are not zeros so that the signal of a particular subcarrier contributed from the long-delay multipath causes influence to the others. If the samples at a particular zero-valued subcarrier from multiple antennas are constructed to form the spatial snapshot, the spatial statistics will contain the spatial information of the multipath with the delays larger than the CP length.

To simplify the analysis, we adopt the assumption in [31]. In [31], it indicates that many outdoor environments have the base station (BS) located higher than the surrounding scatterers, so the received power is concentrated in a very small angular spread. We assume that the useful signals of a particular user arrive at the BS from a single direction of arrival but different from that of the multipath whose delay is larger than the CP duration. Let the $Q\times 1$ spatial snapshot at the mth subcarrier that is used by the vth user can be represented as

$$\begin{aligned}\boldsymbol{g}_m(k) &= \boldsymbol{a}(\theta_S^{(v)})\tilde{X}_m^{(v)}(k)\left[\boldsymbol{H}^{f(v)}_{U(1)}(k)\right]_{m,m} \\ &+ \boldsymbol{a}(\theta_I^{(v)})\sum_{l=N_o^{(v)}}^{N_o^{(v)}+N^{(v)}-1}\tilde{X}_l^{(v)}(k)\cdot\left[\boldsymbol{H}^{f(v)}_{\mathrm{ICI}(1)}(k)\right]_{m,l} \\ &+ \boldsymbol{a}(\theta_I^{(v)})\sum_{l=N_o^{(v)}}^{N_o^{(v)}+N^{(v)}-1}\tilde{X}_l^{(v)}(k-1)\cdot\left[\boldsymbol{H}^{f(v)}_{\mathrm{ISI}(1)}(k)\right]_{m,l}+\boldsymbol{n}'_m(k)\end{aligned} \quad (14)$$

where $\tilde{X}_l^{(v)}(k)$ is the symbol of the kth transmit block after the DFT operation and being mapped to the lth subcarrier. $\theta_S^{(v)}$ and $\theta_I^{(v)}$ denote AOAs of the paths whose time delays are smaller and larger than the duration of the CP, respectively. $\boldsymbol{n}'_m(k)$ is AWGN at the mth subcarrier. The spatial snapshot at the mth subcarrier that is a zero-valued subcarrier can be represented as

$$\begin{aligned}\boldsymbol{g}_m(k) &= \boldsymbol{a}(\theta_I^{(v)})\sum_{l=N_o^{(v)}}^{N_o^{(v)}+N^{(v)}-1}\tilde{X}_l^{(v)}(k)\cdot\left[\boldsymbol{H}^{f(v)}_{\mathrm{ICI}(1)}(k)\right]_{m,l} \\ &+ \boldsymbol{a}(\theta_I^{(v)})\sum_{l=N_o^{(v)}}^{N_o^{(v)}+N^{(v)}-1}\tilde{X}_l^{(v)}(k-1)\cdot\left[\boldsymbol{H}^{f(v)}_{\mathrm{ISI}(1)}(k)\right]_{m,l}+\boldsymbol{n}'_m(k)\end{aligned} \quad (15)$$

Therefore these spatial snapshots can be utilised to estimate the interference correlation matrix. If the criterion (10) is employed to find the beamforming weight vector, the weight vector will form a beam towards to the direction $\theta_S^{(v)}$ of the useful signals and suppress the multipath signals with the AOA $\theta_I^{(v)}$.

On the other hand, the characteristics of the samples at the zero-valued subcarriers are analysed, which will be utilised for the design of the proposed adaptive algorithm. Referring to Fig. 2, it illustrates the effect of the ICI in the frequency domain caused by the long-delay multipath signal which is plotted by using (12) if we transmit a modulation symbol at a subcarrier. The subcarrier is marked with a circle and its index is set to be zero in Fig. 2. The effect of the ICI decreases while the index difference of another subcarrier from this specified modulated subcarrier becomes large. The effect of the ICI because of the long-delayed multipath signal at the mth subcarrier from the data subcarriers of the current block and the previous block of the vth user is

$$\begin{aligned}z^{(q)}_{\mathrm{ICI},m}(k) &= \sum_{l=N_o^{(v)}}^{N_o^{(v)}+N^{(v)}-1}\tilde{X}_l^{(v)}(k)\cdot\left[\boldsymbol{H}^{f(v)}_{\mathrm{ICI}(q)}(k)\right]_{m,l} \\ &+ \sum_{l=N_o^{(v)}}^{N_o^{(v)}+N^{(v)}-1}\tilde{X}_l^{(v)}(k-1)\cdot\left[\boldsymbol{H}^{f(v)}_{\mathrm{ISI}(q)}(k)\right]_{m,l}\end{aligned} \quad (16)$$

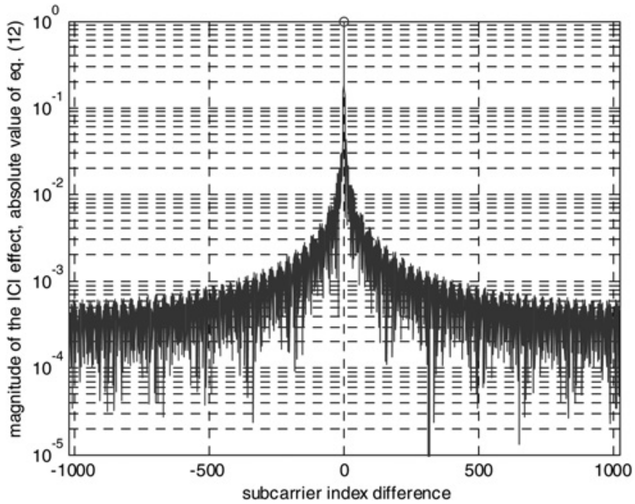

Fig. 2 *Illustration for the effect of the ICI because of insufficient CP, 2048 subcarriers*

Assume $\tilde{X}_l^{(v)}(k)$ is the uncorrelated symbols with zeros mean and equal variance. Although the mth subcarrier is the interested subcarrier, a function is defined as

$$\Upsilon_m = \frac{E\left[\left|\tilde{z}_{\mathrm{ICI},m}^{(q)}(k)\right|^2\right]}{\sigma^{22} + I_m} \quad (17)$$

where σ^2 is the variance of AWGN and I_m is the expectation value of the interference contributed from another user. In (17), the denominator in (17) is invariant with different m. Referring to Fig. 2, in another point of view, the signal level of the long-delay multipath becomes lower if we take the sample at the zero-valued subcarrier far away from the modulated subcarrier. Referring to (17), if we treat the long-delay multipath signal as the interested signal, the SINR of the sample taken at a particular subcarrier becomes smaller while the index difference is large. In the proposed method, the spatial correlation matrix estimation $\tilde{\boldsymbol{R}}_I^{(v)}(k)$ is required. Owing to finite sample number effect, some noisy samples may not be suitable used for the estimation purpose. As the target of the scheme aims to cancel/suppress the long-delay multipath signal and the nature of the signal is approximately fixed during the estimation period, we would like to select the samples with relative larger SINR for the estimation purpose. As indicated in Fig. 2, the scheme would rather select samples at those subcarriers closer to the modulated subcarriers to provide more accurate estimation and achieve better cancelation/suppression performance. Therefore the paper constructs this function (17) to evaluate the SINRs of the available samples in the zero-valued subcarrier region. Referring to Fig. 2, if the index difference of the subcarrier in the zero-valued subcarrier region from the modulated subcarrier region becomes large, the SINR becomes smaller. Therefore we should select the samples at the zero-valued subcarriers with the smaller index difference from the modulated subcarrier region.

A larger value of Υ_m means the sample at subcarrier m can provide better estimation of the interference (plus noise) spatial correlation matrix as the goal is to cancel the multipath signal with long delay. The goal of the proposed algorithm tends to cancel those multipaths with delays larger than the duration of CP while keeping other multipath signals intact. Those multipaths with long delays may have significant power compared with noise and interference from other users. During the estimation process, the channel impulse response is assumed to be fixed and the frequency response matrices are fixed (11)–(13). Note that the large delay multipath signal is fixed while noise and interference from other users have random nature.

Intuitively, we may use all samples at the zero-valued subcarriers to estimate the interference (plus noise) spatial correlation matrix [22]. However, based on the above observation, not all samples at the zero-valued subcarriers should be employed. The main reason is that the samples at these virtual subcarriers have different SINRs. According (17), we would rather select the samples with larger values of Υ_m for the correlation matrix estimation which means the power ratio of the long-delay multipath over the noise plus interference from other users has larger values. By trading off the finite sample effect and the estimation quality related to the value of Υ_m, the suggested number of samples for the following proposed algorithm is revealed in the simulation. We evaluate the efficacy of the sample selection by varying the number of the samples in the simulation.

4 Proposed adaptive algorithm

A new adaptive processing scheme for the calculation of the beamforming weight vector is developed in the section. Note that there are several subcarriers per user in a SC-FDMA symbol with different characteristics. The analysis in Section 3 explains why we select samples to perform the estimation of the correlation matrix. Classical adaptive algorithms cannot be applied directly to solve the beamforming problem. The design of the adaptive algorithm is not straightforward as the special characteristics of the samples should be considered and the available number of samples per SC-FDMA symbol period are different in the estimation of the matrix pencil $\{\tilde{\boldsymbol{R}}_{S+I}^{(v)}(k), \tilde{\boldsymbol{R}}_I^{(v)}(k)\}$. Two sequences with different number of samples are involved. The forms of classical adaptive algorithms do not have one-to-one mapping for direct application to the signals under consideration and the proposed expression does not directly adopt the known iteration methods. For example, it involves how to perform iterations per SC-FDMA symbol. We have to find an efficient update form incorporated into the iteration procedure as the proposed adaptive algorithm for the application under consideration. In [22], the interference-alone (plus noise) spatial correlation matrix is estimated by averaging one block data using all samples at the zero-valued subcarriers in a batch mode. In this manner, the data length of one block may not provide an accurate estimate. Even though one frame data may provide enough data length to obtain accurate estimates in stationary channels, however, the channel gains usually fluctuate in the propagation environments, especially in high mobility scenarios. It may not be a feasible solution.

For aforementioned reason, a new adaptive processing scheme is thus developed as follows. The update formula of the estimated interference spatial correlation matrix of the batch processing-based version may be given as

$$\tilde{\boldsymbol{R}}_I^{(v)}(k) = \eta_I^{\mu}\tilde{\boldsymbol{R}}_I^{(v)}(k-1) + \sum_{l=1}^{\mu} \eta_I^{\mu-l} \boldsymbol{g}_{\boldsymbol{\Psi}^{(v)}(l)}(k)\boldsymbol{g}_{\boldsymbol{\Psi}^{(v)}(l)}^{\mathrm{H}}(k) \quad (18)$$

where η_I is the forgetting factor; μ denotes the snapshot number; and $\boldsymbol{g}_{\boldsymbol{\Psi}^{(v)}(l)}(k)$ denotes the spatial snapshot at the $\boldsymbol{\Psi}^{(v)}(l)$th subcarrier from all antenna outputs of the kth transmit block. $\boldsymbol{\Psi}^{(v)}(l)$ is the lth component in $\boldsymbol{\Psi}^{(v)}$ which is the set of the indexes of the zero-valued subcarriers for the vth user.

Next, the adaptive algorithm is developed to solve the generalised eigenvalue problem for the blind beamforming scheme. It finds the largest generalised eigenvector as the beamforming weight vector in an adaptation fashion. The power method is a well-known iteration method for finding the largest eigenvector of a matrix $\boldsymbol{A}$ [25]. The method for the application to subspace track can be found in [32]. The recursive equation of the power method is given as

$$\boldsymbol{w}(k) = \frac{\boldsymbol{A}\boldsymbol{w}(k-1)}{\|\boldsymbol{A}\boldsymbol{w}(k-1)\|} \quad (19)$$

If initial vector $\boldsymbol{w}(0)$ is not orthogonal to the largest eigenvector of matrix $\boldsymbol{A}$, vector $\boldsymbol{w}(k)$ will converge to the largest eigenvector of matrix $\boldsymbol{A}$. The generalised eigenvalue

IET Commun., 2014, Vol. 8, Iss. 9, pp. 1477–1487
doi: 10.1049/iet-com.2013.0710

problem of matrices $\{\boldsymbol{A}, \boldsymbol{B}\}$ can be represented as $\boldsymbol{A}\boldsymbol{q} = \lambda\boldsymbol{B}\boldsymbol{q}$. Therefore the power method can be applied to solve the generalised eigenvalue problem (1) as $\boldsymbol{B}^{-1}\boldsymbol{A}\boldsymbol{q} = \lambda\boldsymbol{q}$. The update formula is obtained as

$$\boldsymbol{w}_{\text{power}}^{(v)}(k) = \frac{\tilde{\boldsymbol{R}}_{I,\text{power}}^{(v),\text{inv}}(k)\tilde{\boldsymbol{R}}_{S+I,\text{power}}^{(v)}(k)\boldsymbol{w}_{\text{power}}^{(v)}(k-1)}{\left\|\tilde{\boldsymbol{R}}_{I,\text{power}}^{(v),\text{inv}}(k)\tilde{\boldsymbol{R}}_{S+I,\text{power}}^{(v)}(k)\boldsymbol{w}_{\text{power}}^{(v)}(k-1)\right\|} \quad (20)$$

where $\boldsymbol{w}_{\text{power}}^{(v)}(k)$ is the beamforming weight vector of the power-based algorithm; $\|\cdot\|$ denotes the Euclidean norm; $\tilde{\boldsymbol{R}}_{S+I,\text{power}}^{(v)}(k)$ and $\tilde{\boldsymbol{R}}_{I,\text{power}}^{(v),\text{inv}}(k)$ means the estimated signal-plus-interference (plus noise) spatial correlation matrix and the inverse term of the estimated interference (plus noise) spatial correlation matrix for the power-based algorithm, respectively.

From (18), the estimated interference (plus noise) correlation matrix for the adaptive algorithm under development on a per subcarrier basis is modified as

$$\hat{\boldsymbol{R}}_I^{(v)}[l] = \eta_I\hat{\boldsymbol{R}}_I^{(v)}[l-1] + \boldsymbol{g}_{\boldsymbol{\Psi}^{(v)}(l)}(k)\boldsymbol{g}_{\boldsymbol{\Psi}^{(v)}(l)}^{\text{H}}(k) \quad (21)$$

where the index, either l or $l-1$, inside [•] denotes the iteration index of a particular data block. Note that this formula may be treated as a weighting consideration on the samples of the zero-valued subcarriers related the distance to the data subcarrier.

By utilising the numerical method to compute the generalised eigenvector in the form of (19), (20) is thus proposed to calculate the weight vector as the update form and by constructing the mathematical expression in (21), the calculation of the inverse term of the estimated interference plus noise spatial correlation matrix can be performed efficiently through the matrix inversion lemma which is similar to the derivation of the classical recursive least squares (RLS) algorithm, but not the same as the typical problem formulation where the classical RLS can apply. The resulting expression is described in (22) at the processing step 1. The adaptive algorithm based on the power method is described as follows.

Step 1: The spatial snapshot $\boldsymbol{g}_{\boldsymbol{\Psi}^{(v)}(l)}(k)$ at the zero-valued subcarrier is used to update the inverse term of the estimated interference (plus noise) correlation matrix $\hat{\boldsymbol{R}}_I^{(v)}[l]$ by the matrix inverse lemma and is performed ϕ times as

$$\hat{\boldsymbol{R}}_I^{(v),\text{inv}}[l] = \frac{1}{\eta_I}\text{tri} \times \left(\hat{\boldsymbol{R}}_I^{(v),\text{inv}}[l-1] - \frac{\hat{\boldsymbol{R}}_I^{(v),\text{inv}}[l-1]\boldsymbol{g}_{\boldsymbol{\Psi}^{(v)}(l)}(k)\boldsymbol{g}_{\boldsymbol{\Psi}^{(v)}(l)}^{\text{H}}(k)\hat{\boldsymbol{R}}_I^{(v),\text{inv}}[l-1]}{\eta_I + \boldsymbol{g}_{\boldsymbol{\Psi}^{(v)}(l)}^{\text{H}}(k)\hat{\boldsymbol{R}}_I^{(v),\text{inv}}[l-1]\boldsymbol{g}_{\boldsymbol{\Psi}^{(v)}(l)}(k)}\right) \quad (22)$$

where $\hat{\boldsymbol{R}}_I^{(v),\text{inv}}[l]$ means the inverse term of the estimated interference (plus noise) correlation matrix in (21) at a particular received block. The spatial correlation matrices are Hermitian matrices, and the inverse terms of the spatial correlation matrices are also Hermitian matrices. To reduce computational complexity, the upper triangular part of the spatial correlation matrices is calculated and the lower triangular part can be obtained by the Hermitian transpose of the upper triangular part. tri(·) denotes the aforementioned operation.

Step 2: Based on (20), the spatial vectors $\{\boldsymbol{g}_{\boldsymbol{\Gamma}^{(v)}(l)}(k)\}$ at the data subcarriers and the inverse term of the estimated interference (plus noise) correlation matrix are combined to calculate the antenna weight vector at the kth data block as

$$\boldsymbol{w}_{\text{power}}^{(v)}(k) = \frac{\hat{\boldsymbol{R}}_{I,\text{power}}^{(v),\text{inv}}(k)(1/N_B^{(v)})\sum_{l=1}^{N_B^{(v)}}\boldsymbol{g}_{\boldsymbol{\Gamma}^{(v)}(l)}(k)\boldsymbol{g}_{\boldsymbol{\Gamma}^{(v)}(l)}^{\text{H}}(k)\boldsymbol{w}_{\text{power}}^{(v)}(k-1)}{\left\|\hat{\boldsymbol{R}}_{I,\text{power}}^{(v),\text{inv}}(k)(1/N_B^{(v)})\sum_{l=1}^{N_B^{(v)}}\boldsymbol{g}_{\boldsymbol{\Gamma}^{(v)}(l)}(k)\boldsymbol{g}_{\boldsymbol{\Gamma}^{(v)}(l)}^{\text{H}}(k)\boldsymbol{w}_{\text{power}}^{(v)}(k-1)\right\|} \quad (23)$$

where $N_B^{(v)}$ is the number of the data subcarriers used for the estimation of the signal-plus-interference (plus noise) spatial correlation matrix; $\hat{\boldsymbol{R}}_{I,\text{power}}^{(v),\text{inv}}(k)$ means the inverse term of the estimated interference (plus noise) spatial correlation matrix obtained from the power-based algorithm. $N_B^{(v)} < N^{(v)}$ is adopted to reduce the computational complexity. The total computational complexity is only $O(\mu \times Q^2 + N_B^{(v)} \times Q)$. The proposed algorithm is derived based on the numerical procedure in computing the largest generalised eigenvector such that it can perform better than [12]. An approximation is made for the adaptive algorithm in [12] such that the solution may not be equal to the largest generalised eigenvector of the formulated expression asymptotically.

5 Simulation results

In the simulation, the SC-FDMA signal model which is commensurate with the E-UTRA uplink signal model [4] is adopted. The SC-FDMA parameters in the simulation are similar to those in [22]. A linear array of Q antennas with half-wavelength spacing at the base station is employed. The transmission of the system is operated at the carrier frequency 2 GHz. There are 2048 subcarreirs in total. M and N are equal to 2048 and 72 for the DFT and IDFT operations, respectively. The lengths of the CP duration are set as 160 samples (5.2083 µs) for the first block and 140 samples (5.5573 µs) for second to seven block, respectively [4]. To demonstrate the proposed adaptive algorithm being able to cope with the insufficient CP problem, the hilly terrain propagation channel model [32] is adopted with a maximum delay spread of 17.2 µs. The paths whose delays are larger than CP duration have power levels of −6 and −12 dB related to the first path. The modified Jake's model generation method [33] is employed to generate the channel gain $\alpha_i^{(v)}(k)$ with some mobility situation; the channel is assumed to be quasi-stationary. The base station estimates the channel gains of subcarriers for all users perfectly in the demodulation process for simplicity. In OFDM-based systems, the channel gains of subcarriers can be estimated through the use of pilot subcarriers. After applying the beamforming weight vector, the strong co-channel interference is suppressed and the channel gains could be estimated through classical estimation approaches. We suppose that the values of multiuser CFOs have been accurately estimated and are known to the base station for the compensation. The impact of CFO estimation errors on performance will also be shown in the simulation.

In Figs. 3–8, we consider the multiuser scenarios with $Q = 8$ antennas under the insufficient CP problem. There are

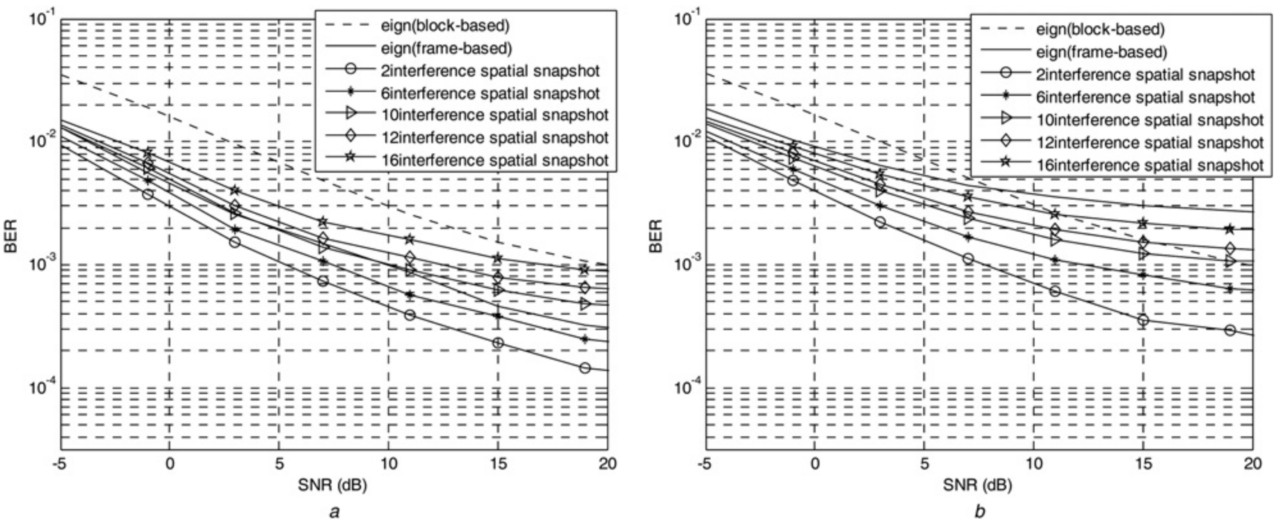

Fig. 3 *BER performance comparison for different numbers of zero-valued subcarriers*

a 4 km/h
b 60 km/h

four users. The first path of each user arrives at an angle of 20°, 0°, −50° and 10°, respectively. The AOA of the path with the delay larger than the CP duration arrives at an angle of 60°, 40°, −15° and −30°, respectively. The angular spread has the range of −15° to 15°. The label 'frame-based' and label 'block-based' in the figures means the spatial correlation matrices are obtained by averaging the signals in one frame and one block, respectively. A frame duration is 10 ms which has 20 time slots. Each time slot has seven blocks (SC-FDMA symbols).

In Figs. 3*a* and *b*, we compare the bit error rate (BER) performance using different number of the zero-valued subcarriers to estimate the interference (plus noise) spatial correlation matrix at a speed of 4 and 60 km/h environment, respectively. η_I is set to be 0.93 and 0.87, respectively. The values are selected according to the simulation experiences for better performance. The weight vectors are calculated by the batch processing method as in [22]. According to the analysis in Section 3, the performance may not be improved by using all the available samples and the samples for the estimation should be selected. As indicated in the result, the performance does not improve in accordance with the increasing number of the samples at the zero-valued subcarriers. This simulation result verifies the analysis in Section 3 and the property that the available samples have varied SINRs and should be selected for estimation is utilised in the proposed adaptive algorithm. The number of the selected samples at the zero-valued subcarriers = 2 is adopted for the following simulation.

In Fig. 4, the performances between the proposed adaptive scheme and the original schemes are compared. The label 'RLS-based' in the figure means the RLS-based adaptive algorithm is implemented for [22]. The original eigenanalysis-based batch processing method by averaging one block in [22] usually has the worst performance at the low speed of the 4 km/h environment. The method by averaging over one frame in [22] has the worst performance at high SNRs in the 60 km/h environment. In either the slowly time-varying environment or the highly time-varying environment, the proposed power method-based scheme is

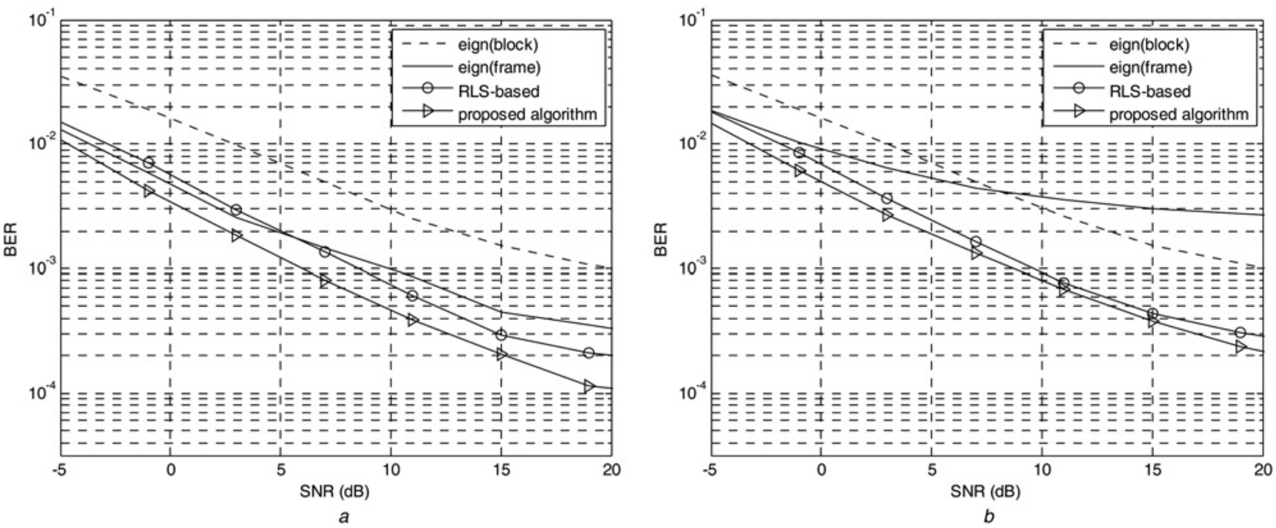

Fig. 4 *BER performance comparison between the proposed adaptive scheme and the original schemes*

a 4 km/h
b 60 km/h

IET Commun., 2014, Vol. 8, Iss. 9, pp. 1477–1487
doi: 10.1049/iet-com.2013.0710

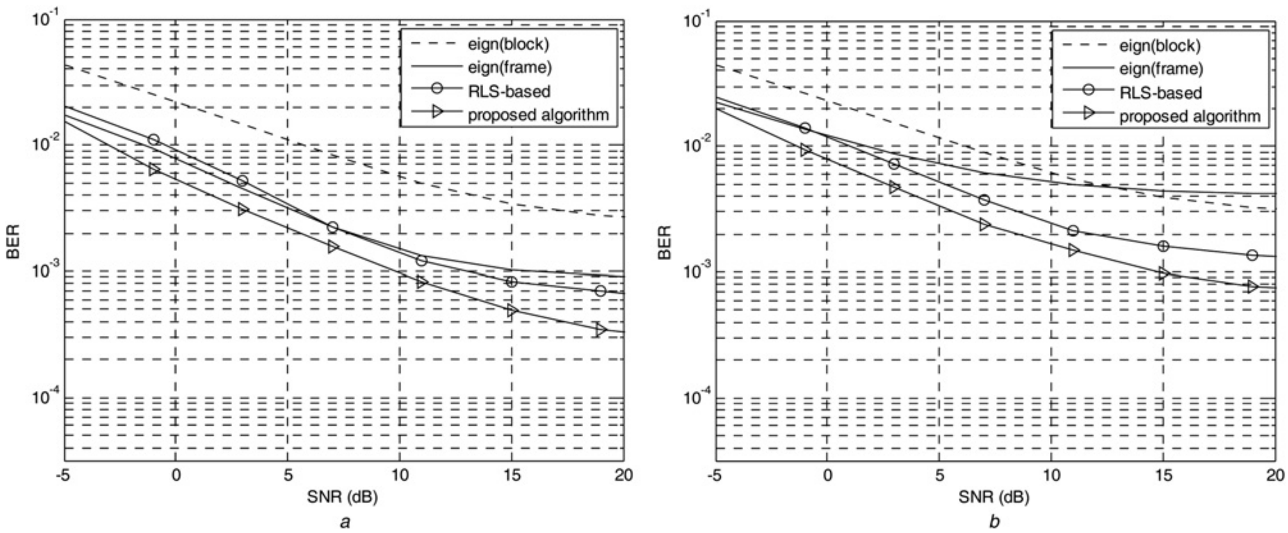

Fig. 5 *BER performance comparison between the proposed adaptive scheme and the original schemes with the CFOs and the strong co-channel interference*

a 4 km/h
b 60 km/h

better than the schemes previously proposed in [22]. In Fig. 5, we add a strong wideband co-channel interferer with a power level of 10 dB above the desire user's direct path and an AOA = −65° as well as the normalised CFO equal to 0.2 in the system. The similar performance trend is observed as in Fig. 4.

In Fig. 6, we consider the situation with existing CFO estimation errors. The simulation is conducted with the same setup as that of the result in Fig. 5. The values of the CFO estimation errors are randomly generated by using uniform distribution within the range in the labels. As revealed in the results, the proposed adaptive beamforming scheme can also work with CFO estimation errors with slight degradation and outperforms the other schemes for comparison.

Finally, to assess convergence characteristics of the proposed adaptive solution for the blind beamforming scheme, an output SINR is used as the performance measure and is defined as

$$\mathrm{SINR} = \frac{\boldsymbol{w}^{\mathrm{H}}\left[\sum_{\left\{i|d_i^{(v)} \le N_g\right\}} \left|P_i^{(v)} \alpha_i^{(v)}(k)\right|^2 \boldsymbol{a}(\theta_i^{(v)})\boldsymbol{a}^{\mathrm{H}}(\theta_i^{(v)})\right]\boldsymbol{w}}{\boldsymbol{w}^{\mathrm{H}}\left[\sum_{\left\{i|d_i^{(v)} > N_g\right\}} \left|P_i^{(v)} \alpha_i^{(v)}(k)\right|^2 \boldsymbol{a}(\theta_i^{(v)})\boldsymbol{a}^{\mathrm{H}}(\theta_i^{(v)}) + \sigma^2 \boldsymbol{I}\right]\boldsymbol{w}} \tag{24}$$

The term in the bracket of the numerator comprises the paths whose time delays are smaller than the duration of the CP. The term in the bracket of the denominator comprises the paths whose time delays are larger than the duration of the CP and AWGN. A plot of BER against CP length deviation from the standard setting of [34] (160 samples for first

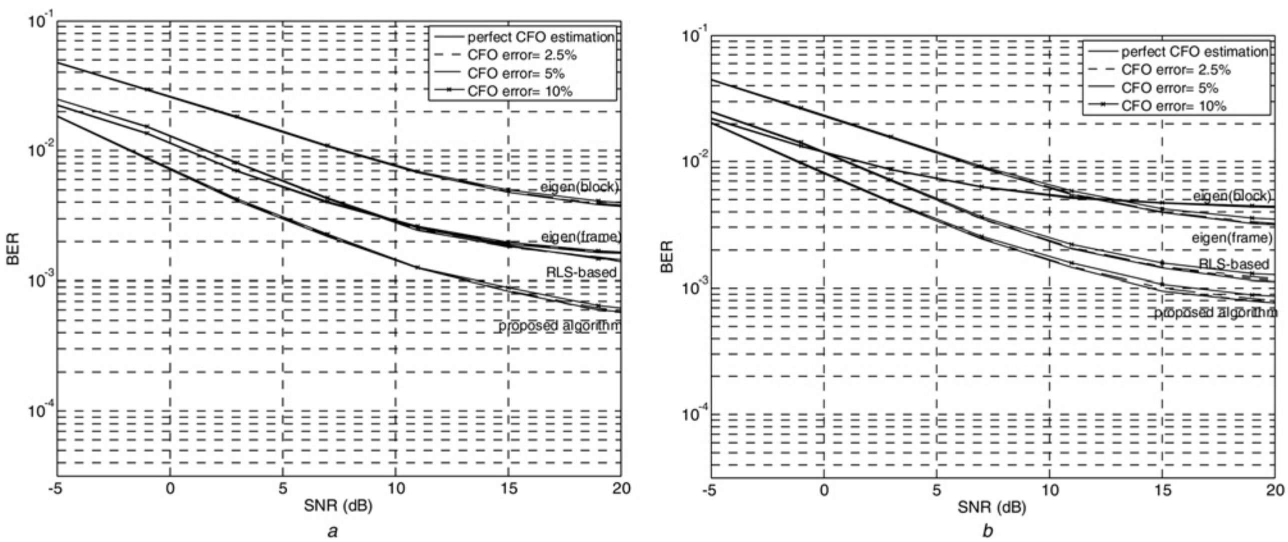

Fig. 6 *BER performance comparison between the proposed adaptive scheme and the original schemes under the CFOs and the co-channel interference scenarios with CFO estimation errors*

a 4 km/h
b 60 km/h

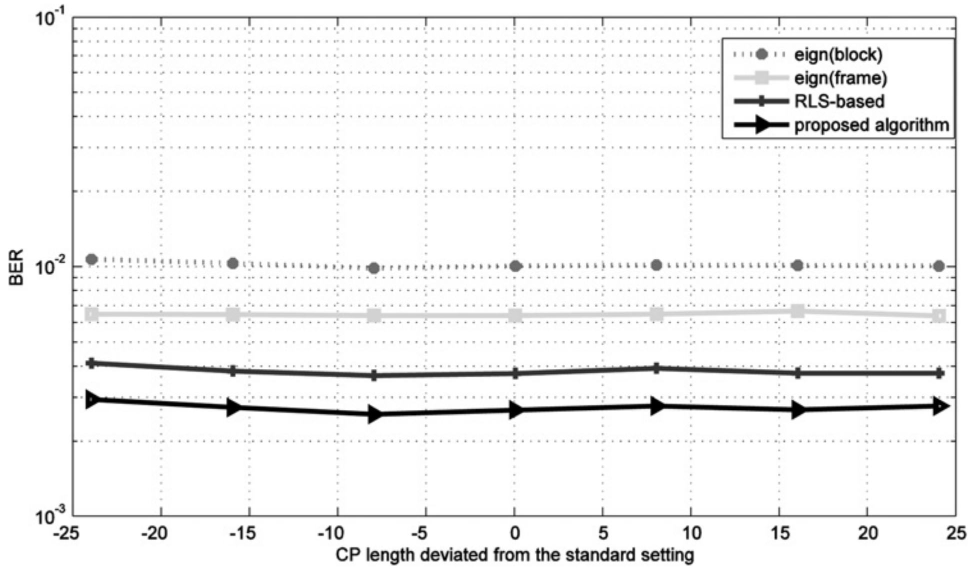

Fig. 7 *BER performance against CP length deviated from standard setting of [4, 34] with SNR = 3 and mobile speed 60 km/h*

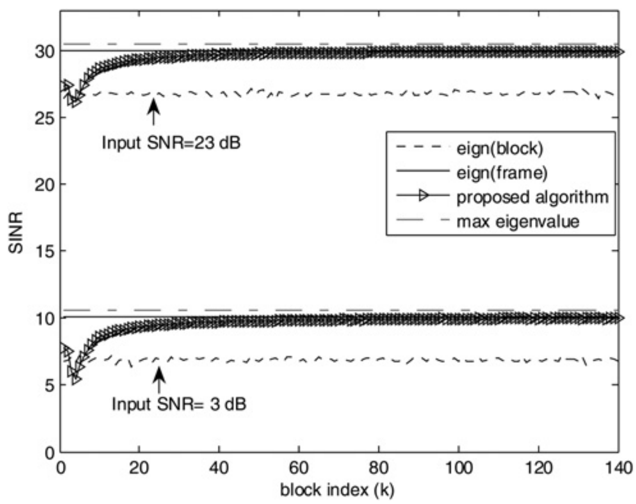

Fig. 8 *Convergence curves in terms of output SINRs*

block and 140 samples for second to seven block)are shown in Fig. 7, the SNR and the mobile speed are fixed as SNR = 3 dB and 60 km/h, respectively. In Fig. 8, the output SINRs defined in (24) are plotted to show the convergence characteristics of the proposed scheme in a stationary environment at input SNR = 3 dB and 23 dB, respectively. It shows convergence and is very close to the optimal value.

6 Conclusions

In this paper, the capability in suppressing the long-delay multipath signal is verified for the blind beamforming scheme with insufficient CP problem in SC-FDMA systems. The analysis is also utilised to design an adaptive algorithm. The adaptive processing scheme for the blind beamforming problem is developed based on the power method. The adaptive algorithm is developed to find the beamforming weight vector in a tracking manner on a per SC-FDMA symbol basis without using reference signals. The adaptive processing scheme can achieve competitive performance under insufficient CP scenarios even with the strong wideband co-channel interferer and the CFO estimation errors. The simulation results show that the power method-based adaptive blind beamforming algorithm can achieve better performance to cope with the time-varying communication environments. Its computational complexity is only $O(\mu \times Q^2 + N_B^{(v)} \times Q)$.

7 Acknowledgment

This work was supported by the National Service Council, Taiwan, Republic of China, under contract NSC 102-2221-E-008-005.

8 References

1 Tanno, M., Kishiyama, Y., Miki, N., Higuchi, K., Sawahashi, M.: 'Evolved UTRA – physical layer overview'. Proc. IEEE Signal Process. Advances in Wireless Communications, June 2007, pp. 1–8
2 Myung, H.G., Lim, J., Goodman, D.J.: 'Single carrier FDMA for uplink wireless transmission', *IEEE Veh. Technol. Mag.*, 2006, **1**, (3), pp. 30–38
3 Cimini, L.Jr.: 'Analysis and simulation of a digital mobile channel using orthogonal frequency division multiplexing', *IEEE Trans. Commun.*, 1985, **33**, (7), pp. 665–675
4 '3GPP Technical Specification 36.211', Evolved Universal Terrestrial Radio Access (E-UTRA), *Physical channels and modulation* Available at: http://www.3gpp.org
5 Sun, Y., Tong, L.: 'Channel equalization for wireless OFDM systems with ICI and ISI'. Proc. IEEE Int. Conf. Commun., June 1999, vol. 1, pp. 182–186
6 Suyama, S., Hara, Y., Suzuki, H., Kamio, Y., Fukawa, K.: 'A maximum likelihood OFDM receiver with smoothed FFT-window for large multipath delay difference over the guard interval'. Proc. IEEE Vehicular Technology Conf., May 2002, vol. 3, pp. 1247–1251
7 Zamiri-Jafarian, H., Khoshbin, H., Pasupathy, S.: 'Time-domain equalizer for OFDM systems based on SINR maximization', *IEEE Trans. Commun.*, 2005, **53**, (6), pp. 924–929
8 Daly, D., Heneghan, C., Fagan, A.D.: 'Minimum mean-squared error impulse response shortening for discrete multitone transceivers', *IEEE Trans. Signal Process.*, 2004, **52**, (1), pp. 301–306
9 Lim, C., Chang, Y., Cho, J., Joo, P., Lee, H.: 'Novel OFDM transmission scheme to overcome caused by multipath delay longer than cyclic prefix'. Proc. IEEE Vehicular Technology Conf., June 2005, vol. 3, pp. 1763–1767
10 Hara, S., Nishikawa, A., Hara, Y.: 'A novel OFDM adaptive antenna array for delayed signal and Doppler-shifted signal suppression'. Proc. IEEE Int. Conf. Communications, June 2001, vol. 7, pp. 2302–2306

doi: 10.1049/iet-com.2013.0710

11 Budsabathon, M., Hara, Y., Hara, S.: 'Optimum beamforming for pre-FFT OFDM adaptive antenna array'. Proc. IEEE Wireless Communications Net. Conf., March 2003, vol. 1, pp. 32–37
12 Chen, Y.F., Wang, C.S.: 'Adaptive antenna arrays for interference cancellation in OFDM communication systems with virtual carriers', *IEEE Trans. Veh. Technol.*, 2007, **56**, (4), pp. 1837–1844
13 Li, Y., Sollenberger, N.R.: 'Adaptive antenna arrays for OFDM systems with cochannel interference', *IEEE Trans. Commun.*, 1999, **47**, (2), pp. 217–229
14 Kapoor, S., Marchok, D.J., Huang, Y.-F.: ' Adaptive interference suppression in multiuser wireless OFDM systems using antenna arrays', *IEEE Trans. Signal Process.*, 1999, **47**, (12), pp. 3381–3391
15 Zhang, H., Li, Y.: 'Clustered OFDM with adaptive antenna arrays for interference suppression', *IEEE Trans. Wirel. Commun.*, 2004, **3**, (6), pp. 2189–2197
16 Kim, C.K., Lee, K., Cho, Y.S.: 'Adaptive beamforming algorithm for OFDM systems with antenna arrays', *IEEE Trans. Consum. Electron.*, 2000, **46**, (4), pp. 1052–1058
17 Huang, Y.-R., Fung, C.C., Wong, K.T.: 'Interference suppression for OFDM systems with insufficient guard interval using null subcarriers', *IEEE Signal Process. Lett.*, 2009, **16**, (11), pp. 929–932
18 Miyajima, T., Ding, Z.: 'Subcarrier nulling algorithms for channel shortening in uplink OFDMA systems', *IEEE Trans. Signal Process.*, 2012, **60**, (5), pp. 2374–2385
19 Hayashi, K., Kojima, T., Sakai, H.: 'A new beamforming method for single carrier modulation system with cyclic prefix'. Proc. Sixth Baiona Workshop on Communications, September 2003, pp. 75–80
20 Leon, W.S., Liang, Y.C., Zeng, Y., Xu, C.: 'Channel delay management with statistical pre-filtering for single carrier cyclic prefix transmissions'. Proc. IEEE Vehicular Technology Conf., April 2007, pp. 1766–1770
21 Dessouky, M.I., Sallam, B.M., Shawki, F., Abd El-Samie, F.E.: 'Uplink single-carrier frequency division multiple access system with joint equalisation and carrier frequency offsets compensation', *IET Commun.*, 2011, **5**, (4), pp. 425–433
22 Liu, C.Y., Chen, Y.F., Li, C.P.: 'Blind beamforming schemes in SC-FDMA systems with insufficient cyclic prefix and carrier frequency offset', *IEEE Trans. Veh. Technol.*, 2009, **58**, (9), pp. 4848–4859
23 Cao, Z., Tureli, U., Yao, Y.-D.: 'Low-complexity orthogonal spectral signal construction for generalized OFDMA uplink with frequency synchronization errors', *IEEE Trans. Veh. Technol.*, 2007, **56**, (3), pp. 1143–1154
24 Kleider, J.E., Ma, X., Steenhoek, C.: 'OFDM subcarrier interference cancellation for non-linear PA distortion'. IEEE 2009 Military Communications Conf., MILCOM 2009, 2009, pp. 1–7
25 Golub, G.H., Van Loan, C.F.: 'Matrix Computations' (Johns Hopkins Univ. Press, Baltimore, MD, 1996)
26 Morgan, D.R.: 'Downlink adaptive array algorithms for cellular mobile communications', *IEEE Trans. Commun.*, 2003, **51**, (3), pp. 476–488
27 Yang, J., Xi, H., Yang, F., Zhao, Y.: 'RLS-based adaptive algorithms for generalized eigen-decomposition', *IEEE Trans. Signal Process.*, 2006, **54**, (4), pp. 1177–1188
28 Tanaka, T.: 'Fast generalized eigenvector tracking based on the power method', *IEEE Signal Process. Lett.*, 2009, **16**, (11), pp. 969–972
29 Yao, Y., Giannakis, G.B.: 'Blind carrier frequency offset estimation in SISO, MIMO, and multiuser OFDM systems', *IEEE Trans. Commun.*, 2005, **53**, (1), pp. 173–183
30 Chen, S., Zhu, C.: 'ICI and ISI analysis and mitigation for OFDM systems with insufficient cyclic prefix in time-varying channels', *IEEE Trans. Consum. Electron.*, 2004, **50**, (2), pp. 78–83
31 Zhang, Y.J., Letaief, K.B.: 'An efficient resource-allocation scheme for spatial multiuser access in MIMO/OFDM systems', *IEEE Trans. Commun.*, 2005, **53**, (1), pp. 107–116
32 Badeau, R., David, B., Richard, G.: 'Fast approximated power iteration subspace tracking', *IEEE Trans. Signal Process.*, 2005, **53**, (8), pp. 2931–2941
33 Zheng, Y.R., Xiao, C.: 'Improved models for the generation of multiple uncorrelated Rayleigh fading waveforms', *IEEE Commun. Lett.*, 2002, **6**, (6), pp. 256–258
34 '3GPP Technical Specification 45.005', *Evolved Universal Terrestrial Radio Access (E-UTRA), Radio transmission and reception* Available at: http://www.3gpp.org